

SIMULATED BEAM-BEAM LIMITS FOR CIRCULAR LEPTON AND HADRON COLLIDERS

K. Ohmi, KEK, 1-1 Oho, Tsukuba, 305-0801, Japan

Abstract

The beam-beam limit is one of the most important collider parameters. For lepton colliders the empirical tune shift limits are higher than for hadron colliders, which has been attributed to strong radiation damping. The beam-beam limit in hadron colliders, like the LHC, can be affected by noise. For future higher-energy colliders, like FCC-hh or SppC, the limit can be higher or lower, in the presence of still rather weak synchrotron radiation. For circular lepton colliders, like DAFNE, SuperKEKB, FCC-ee or CepC, the effect of large Piwinski angle, and crab waist, as well as the dependence of the beam-beam limit on the number of interaction points are important questions. This presentation reviews the state of the art in weak-strong, quasi-strong-strong and strong-strong beam-beam simulations and reports the various dependencies of the simulated beam-beam limit on the aforementioned parameters.

INTRODUCTION

When two beams collides, each beam experiences electro-magnetic field induced by the other beam. Electro-magnetic field, which is formed in transverse plane for a relativistic beam, is represented by 2 dimensional potential. The beam-beam force is quite nonlinear for the betatron amplitudes. The nonlinear beam-beam force causes emittance growth. Nonlinear interaction between two beams causes coherent motion and collective emittance growth. They limit the performance of colliders.; so called the beam-beam limit.

There are several differences in lepton and proton colliders. Electron/positron beams experience the radiation damping with ~10 ms. Flat beam collision is popular in lepton colliders, while round beam collision is popular in proton colliders. Beta function especially in vertical at Interaction Point is smaller than bunch length, hourglass effect is serious in lepton colliders. We discuss typical beam-beam limit processes for lepton and hadron colliders. Crossing angle is key point in recent colliders. In recent lepton colliders, a large crossing angle is adopted with couple to crab waist scheme. A large crossing angle is adopted in proton colliders, and the luminosity controlled by crab cavities.

Tune shift due to the collision force is a measure of the beam-beam limit.

$$\xi = \Delta\nu_{x(y)} = \frac{Nr_0}{2\pi\gamma} \frac{\beta_{x(y)}}{\sigma_{x(y)}(\sigma_x + \sigma_y)} R(\sigma_z/\beta_y, \theta_c \sigma_z/\sigma_x) \quad (1)$$

where R is form factor for hourglass and crossing angle. $R = 1$ for $\sigma_z \ll \beta_y$ and $\theta_c \ll \sigma_x/\sigma_z$. The tune shift is limited for emittance growth and/or coherent motion due to the beam-beam interaction. Luminosity is also limited under the situation.

Simulation for the beam-beam interactions are one and only tool to study the beam-beam limit quantitatively. Two types of simulations have been performed to study the beam-beam effects. One is based on the weak-strong model. Second is based on the strong-strong model. The simulation methods are introduced in next section, and results for lepton and hadron colliders were presented following sections.

SIMULATION METHODS

Weak-Strong Model

The target beam is represented by a Gaussian charge distribution in transverse. For Gaussian charge distribution in transverse plane, colliding beam particle experiences a force given by Bassetti-Erskine formula [1, 2],

$$\begin{aligned} \Delta p_y + i\Delta p_x &= e^{-H_{bb}}(p_y + ip_x) \\ &= \frac{2N_b r_e}{\gamma} \sqrt{\frac{2\pi}{\sigma_x^2 - \sigma_y^2}} \left[w\left(\frac{x + iy}{\sqrt{2(\sigma_x^2 - \sigma_y^2)}}\right) \right. \\ &\quad \left. - \exp\left(-\frac{x^2}{2\sigma_x^2} - \frac{y^2}{2\sigma_y^2}\right) w\left(\frac{\frac{\sigma_y}{\sigma_x}x + \frac{\sigma_x}{\sigma_y}y}{\sqrt{2(\sigma_x^2 - \sigma_y^2)}}\right) \right], \quad (2) \end{aligned}$$

where N_b is the number of particles contained in a fixed charge distribution and $w(x)$ is the complex error function.

In recent e^+e^- colliders, the vertical beta function is squeezed smaller than the bunch length, $\beta_y^* < \sigma_z$. Collision with crossing angle is popular. In hadron colliders, crossing angle is used to avoid parasitic interactions. The bunch length is necessarily taken into account in simulations. A target bunch is sliced along longitudinal, and macro-particles are tracked by repeating collisions with slice by slice along z , [3, 4].

Strong-Strong Model

Both of the colliding beams are represented by macro-particles in strong-strong model. Simulation is performed so that the distributions of two beams are self-consistent. Two methods for beam distribution are used. One is the method in which potential solver on meshed space is used. It is possible to treat collision of arbitrary two beam distributions self-consistently. There are several codes and works on the strong-strong simulations [5–11]. The other is that the beam distribution is approximated by Gaussian which is soft-Gaussian approximation [12]. Rms beam size of macro-particles is calculated in every collision and beam-beam kick is calculated by Eq(2).

Since PIC based simulation is more popular, we discuss a potential solver more detail. Electro-magnetic field is

induced in the transverse plane for a relativistic beam. Even in a non-relativistic beam, the field is in the transverse plane, for the case that the bunch length is larger than the transverse beam size in most cases. Two dimensional Poisson solver is used to calculate the electro-magnetic field in the transverse plane.

Green function in the open boundary condition is expressed by

$$G(x, y) = \frac{1}{2} \ln(x^2 + y^2). \quad (3)$$

Potential is obtained using Green function by

$$\phi(\mathbf{x}) = -\frac{Nr_e}{\gamma} \int d\mathbf{x}' G(\mathbf{x} - \mathbf{x}') \rho(\mathbf{x}') \quad (4)$$

Fast Fourier Transformation (FFT) is used to solve the potential,

When two beams are separated by an certain offset, it is better to choose the mesh area individually. The 2-D Potential of an area where separated from a constant offset \mathbf{x}_0 is calculated by the shifted Green function [8], $G(\mathbf{x} - \mathbf{x}' - \mathbf{x}_0) \rho(\mathbf{x}')$. Collision with a large Piwinski angle becomes popular in recent colliders. One head and the other tail parts of bunches collide with an offset. The shifted Green function is used in this collision simulation.

Statistical noise of macro-particles induces an fluctuation in potential calculated by PIC. or center of Bassetti-Erskine formula. The unphysical emittance growth by the noise is cared in the strong-strong simulation.

In both of the simulations, arc transformation is represented by 6×6 revolution matrix start from IP to IP. Symplectic $\times 6$ matrix contains 21 parameters. 9 of them are $\alpha_i, \beta_i, \nu_i, i = x, y, z$. $\alpha_{xy} = 0$ at IP. Ideal collider model is represented by these 9 parameters. Other 12 parameters are related to errors; 4 parameters characterize x-y coupling $r_1 - r_4$, 4 dispersion η_{xy} and η'_{xy} , and 8 parameters characterize xz and yz tilt, ζ_{xy} and ζ'_{xy} [13]. Chromaticity is expressed by a generating function [14]. Simulations considering full lattice information are being done [15].

BEAM-BEAM LIMIT IN LEPTON COLLIDERS

Lepton colliders operated till now have adopted collision scheme without crossing angle or with a small crossing angle. For example, PEP-II and LEP adopted collision without crossing angle, while KEKB, BEPC-II, DAFNE adopted collision with small crossing angle, where Piwinski angle in them is $\theta_c \sigma_z / \sigma_x \leq 1$.

Large crossing angle scheme is proposed in Hadron colliders at fast [16, 17], and then it is being adopted in lepton collision wit combination of crab waist scheme [18]. DAFNE was changed to the large crossing angle scheme $\theta_c \sigma_z / \sigma_x = 2$ in 2007 [19]. SuperKEKB adopted the scheme $\theta_c \sigma_z / \sigma_x = 20$ though without crab waist. FCC-ee and CepC is going to the large crossing angle scheme in their design.

The beam-beam limit of the two schemes is discussed using parameters based on FCC-ee-HZ production. Emittance and beta function at IP are $\varepsilon_{x/y} = 0.61$ nm/1 pm

and 1/0.002 m, respectively. The damping time is $\tau_{xy}/T_0 = 150$ turns. Computer codes named ‘‘BBWS’’ and ‘‘BBSS’’ [6, 20] developed by the author is used for the weak-strong and strong-strong, respectively.

Luminosity is calculated by overlap of two beam distributions in the simulations. The equilibrium beam-beam tune shift is evaluated from the luminosity using,

$$\xi_L = \frac{2r_e \beta^* L}{N_e \gamma f_{rep}}. \quad (5)$$

This formula is based on the vertical tune shift given by the design horizontal size σ_x and simulated luminosity. We call this beam-beam parameter in this paper.

Beamstrahlung is removed to extract fundamental beam-beam limit of each collision scheme.

Collision with Small Crossing Angle

The beam-beam limit for small crossing angle was discussed for KEKB [20, 21]. The beam-beam tune shift increases to $\xi_L \approx 0.2$ for zero crossing angle at the horizontal tune slightly upper of half integer, where the damping time was 4000 turns for KEKB.

Bunch population is scanned for 1.0, 1.5, 2.0, 3.0, 4.0 \times of the design value, $N_e = 8 \times 10^{10}$. Beam-beam tune shift is calculated using the beam size geometrically, taking into account hourglass effect and crossing angle. We call it nominal tune shift. The nominal beam-beam tune shift ξ_0 is 0.279 and 0.247 without and with crossing angle, respectively, at the design bunch population, $N_e = 8 \times 10^{10}$. The nominal tune shift ξ_0 is proportional to N_e . Bunch population is scanned for 0.75, 1.0, 1.5, 2.0, 3.0, 4.0 \times of the design value, $N_e = 6, 8, 12, 16, 24, 32 \times 10^{10}$. Crossing angle is 0 and 6.1 mrad; Piwinski angle $\theta_c \sigma_z / \sigma_x = 0$ and 0.5 ($\sigma_z = 2$ mm).

Weak-Strong Simulation Figure 1 shows evolution of the beam-beam parameter for without and with crossing angle given by the weak-strong simulation. Figure 2 shows the beam-beam parameter as function of the nominal tune shift. The beam-beam parameter is roughly equal to the nominal tune shift $\xi_L \approx \xi_0$ for $\xi_0 \leq 0.5$, and is saturated at around 0.55.

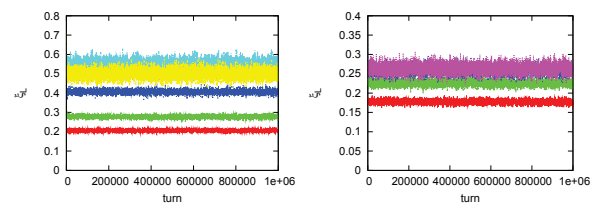


Figure 1: Evolution of the tune shift evaluated by luminosity in weak-strong simulation. Left and right plots are obtained for w/o and w crossing angle, respectively.

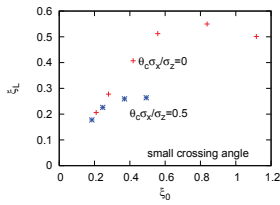


Figure 2: beam-beam parameter as function of the nominal tune shift.

The beam lifetime is another limitation. Figure 3 shows equilibrium distribution of vertical direction. Beam lifetime for zero crossing angle is evaluated as shown in Figure 4. For $\xi_0 < 0.5$, lifetimes is not serious. The weak-strong simulation demonstrates very high beam-beam parameter $\xi_L \approx 0.55$ in the collision without crossing angle.

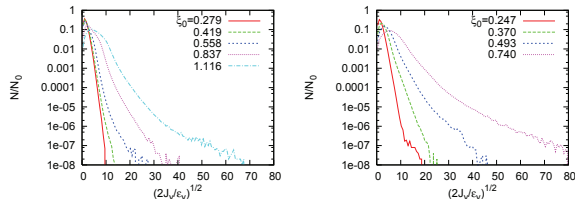


Figure 3: Beam halo distribution in vertical.

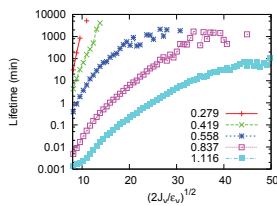


Figure 4: Beam lifetime determined by vertical aperture.

Strong-Strong Simulation Figure 5 shows evolution of the beam-beam parameter and vertical beam size. The beam-beam parameter is saturated at $\xi_L \approx 0.36$ and is unstable for $\xi_0 \geq 0.556$. Vertical beam size, which oscillate, reflects to the behavior of the beam-beam parameter. Variation of the beam sizes is simultaneous and synchronized for both of electron and positron beam; it is “not” quadrupole oscillation. Horizontal size is stable and is somewhat smaller than the design value due to the dynamic beta/emittance effect. Figure 11 shows evolution of the beam-beam parameter given by soft-Gaussian strong-strong simulation. The beam-beam parameter is saturated at $\xi_L \approx 0.5$, closed to the result of the weak-strong simulation. It is discussed that Gaussian approximation is doubtful in extreme condition of the collision [21].

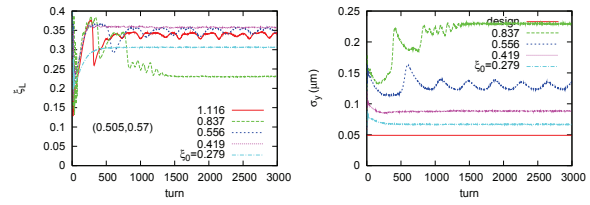


Figure 5: Evolution of the beam-beam parameter and vertical beam size given by strong-strong simulation.

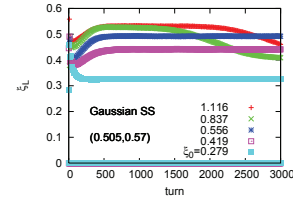


Figure 6: Evolution of the beam-beam parameter given by Gaussian strong-strong simulation.

Collision with Large Crossing Angle and Crab Waist

We study collision with a large Piwinski angle $\theta_c \sigma_z / \sigma_x = 2$. Half crossing angle and bunch length are chosen $\theta_c = 20$ mrad and $\sigma_z = 2.4$ mm, respectively. Crab waist sextupole is set to 20 for $1/2\theta_c = 25$.

Weak-Strong Simulation Figure 7 shows evolution of the beam-beam parameter and its as function of the nominal tune shift with crab waist. The beam-beam parameter is lower without crab waist. The beam-beam parameter with and without crab waist is plotted in the right plot. The beam-beam parameter is saturated around $\xi_L \approx 0.6$ with crab waist, while 0.1 without crab waist. Vertical halo distribution and lifetime for crab waist collision is shown in Figure 8. The lifetime grows worse at $\xi_0 \geq 0.359$ Those without crab waist is worse.

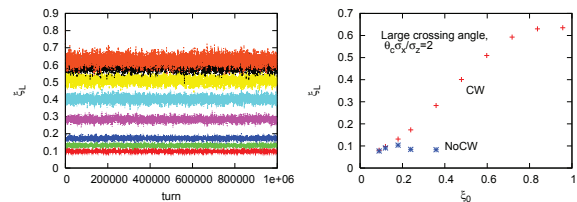


Figure 7: Evolution of the beam-beam parameter (left). Beam-beam parameter as function of the nominal tune shift given by weak-strong simulation.

Strong-Strong Simulation Figure 9 shows evolution of the beam-beam parameter and $\langle xz \rangle$ given by strong-strong simulation. Tune operating point is (0.513,0.57). The beam-beam parameter is now saturated at around $\xi_L \approx 0.15$. For

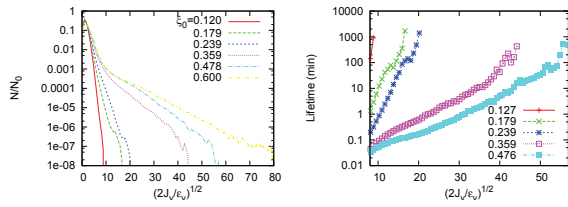


Figure 8: Beam halo distribution in vertical and lifetime.

high nominal tune shift $\xi_0 \geq .239$, luminosity oscillates turn-by-turn. $\langle xz \rangle$, which also oscillates, seems the source of the beam-beam limit. $\langle xz \rangle$ oscillates in phase for two beam.

Figure 10 shows evolution of the beam-beam parameter for different conditions. Left plot depicts that for two limes longer damping time ($\tau_x/T_0 = 300$ turns) and right plot depicts at operating point (0.54,0.57), ($\tau_x/T_0 = 150$ turns). For slower damping time, coherent oscillation is seen at $\xi_0 = 0.12$. The coherent oscillation is seen in every x_0 at the operating point (0.54,0.57). Chromaticity $dv_{x,y}/d\delta = 5$ somewhat suppresses the oscillation, but does not work perfect.

Figure 11 shows the beam-beam parameter for Gaussian strong-strong at tune (0.513,0.57). The beam-beam parameter oscillates turn-by-turn, though not seen in the left plot. (the luminosity is calculated every 10 turns.) $\langle xz \rangle$ oscillation is depicted in the right plot.

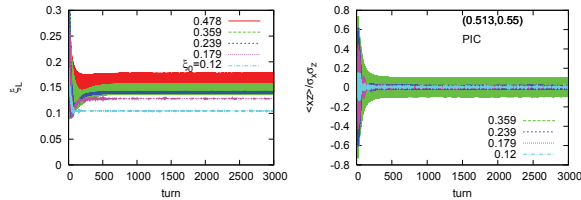


Figure 9: Evolution of the beam-beam parameter given by strong-strong simulation.

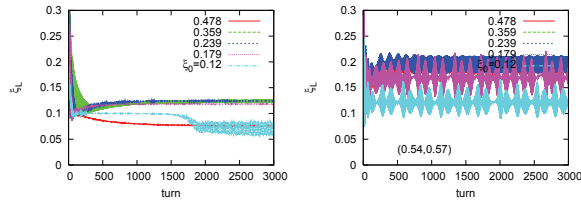


Figure 10: Evolution of the beam-beam parameter for the slower damping time $\tau/T_0 = 600$ turns.

BEAM-BEAM LIMIT IN HADRON COLLIDER

In hadron colliders, the radiation damping time is very long, 1 day (10^9 turns) for LHC and 1 hour (10^7 turns) for FCC-hh. We discuss the beam-beam limit as luminosity degradation/emittance growth rate due to the beam-beam

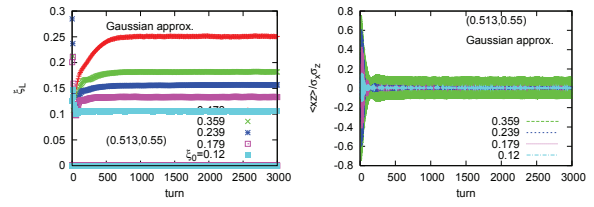


Figure 11: Evolution of the beam-beam parameter given by Gaussian strong-strong simulation.

interaction. An index of the luminosity decrement is $\Delta L/L_0 = 10^{-9}/\text{turn}$ (one day for LHC).

Weak-Strong Simulation Weak-strong simulation is free from the statistical noise. Weak-strong simulation is better to study the beam-beam limit at high tune shift at present, though the model may miss some kinds of luminosity degradation mechanism. Figure 12 shows luminosity decrement for LHC given by weak-strong simulation. Beams collide at 2-IP without crossing angle. The luminosity decrement is very small at the beam-beam tune shift in LHC operation. This figure indicates that tune shift limit is $\xi = 0.2$.

Figure 13 shows the luminosity decrement for finite crossing angle, where Piwinski angle $\theta_{cr,s} \sigma_z / \sigma_x = 0.89$. The tune shift limit is seen $\xi_{tot} = 0.04, 0.02/\text{IP}$ in the presence of the crossing angle.

There are various mechanisms for the luminosity degradation. Detailed study will be published in Ref. [22]. Important points are summarized as

- Betatron resonances with a considerable width exist.
- Beam-beam force depends on z for example due to crossing angle.
- Betatron amplitude satisfying the resonance conditions modulate due to synchrotron motion.

Collision with crossing angle comes under this conditions. Collision with offset does not come, but the offset collision with chromaticity does come.

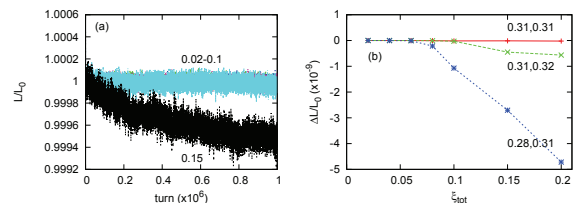


Figure 12: Luminosity decrement for LHC. Picture (a) shows the luminosity evolution for various values of $\xi_{tot} = 2\xi/\text{IP}$. Picture (b) summarizes the luminosity decrement per turn as a function of the total beam-beam parameter ξ_{tot} at three different working points in the tune plane.

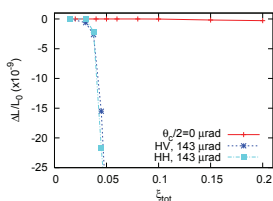


Figure 13: Luminosity decrement as a function of total tune shift for collision with or without a crossing angle of 286 μrad .

Strong-Strong Simulation It is serious problem that a statistical noise for macro-particle number causes artificial emittance growth in strong-strong simulation for hadron colliders. The emittance growth rate due to a collision offset fluctuation Δx is estimated by [22]

$$\frac{\Delta \varepsilon}{\varepsilon} = -\frac{\Delta L}{L} \approx \left(\xi \frac{\Delta x}{\sigma_r} \right)^2 \times 21.7. \quad (6)$$

Figure 14 shows the luminosity decrements as function of the beam-beam tune shift. Two types of points are given for difference macro-particle numbers. Offset fluctuation is $\Delta x \approx \sigma_x / \sqrt{N_{mp}}$. The simulation is PIC based one. Tune is $(\nu_x, \nu_y) = (64.32, 59.31)$ and beams collide at 2-IP with super-periodicity two. The lines are given by Eq.(6). The strong-strong simulation agrees with the formula at $\xi < 0.015/\text{IP}$, but disagrees at $\xi = 0.02/\text{IP}$. It is open question that there is some effects only seen in strong-strong simulation, or the discrepancy of the factor two is not serious. Anyway we do not expect very high tune shift in proton collider. There are other luminosity limitations, for example parasitic interaction, dynamic aperture/lattice, real noise.

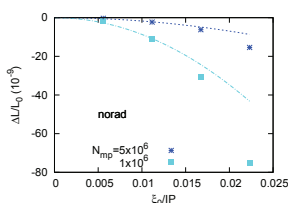


Figure 14: Luminosity decrements depending on macro-particle statistics (BBSS). Left and right plots are the rate without and with synchrotron radiation.

SUMMARY

Various collision schemes are proposed and examined in recent circular lepton/proton colliders. They are collision with/without crossing angle, small/large crossing angle and crab waist. The beam-beam limit in the collision schemes was discussed using weak-strong and strong-strong simulations.

Lepton Colliders Weak-strong simulation gave very high beam-beam parameter $\xi_L > 0.5$ for collision without crossing angle and with combination of crossing angle

and crab waist. Strong-strong simulations gave lower beam-beam parameter; $\xi_L = 0.36$ for zero crossing angle collision and $\xi_L = 0.15$ for crab waist collision. The beam-beam limit is caused by collective emittance growth for zero crossing angle collision and coherent motion in x-z tilt $\langle xz \rangle$ for crab waist collision.

Proton Colliders Weak-strong simulation gave very high beam-beam parameter $\xi > 0.2$ for collision without crossing angle. Crossing angle induces resonances which results beam-beam limit at $\xi = 0.02 \times 2$ IP Strong-strong simulation is hard for numerical noise in high beam-beam tune shift $\xi > 0.02/\text{IP}$. There may be strong-strong effects between $0.02 < \xi < 0.3$.

The author thanks fruitful discussions with Drs. M. Benedikt, X. Buffet, Y. Cai, W. Chou, K. Oide, T. Pieloni, J. Qiang, D. Shatilov, Y. Zhang, D. Zhou, F. Zimmermann.

REFERENCES

- [1] M. Bassetti and G. Erskine, Tech. Rep. ISR TH/80-06, CERN (1980).
- [2] K. Takayama, Lett. al nuvo cimento 34, 190 (1982).
- [3] V. V. Danilov et al., Proceedings of workshop on beam-beam and beam radiation interactions, UCLA, May 13-16 1, 1 (1991).
- [4] K. Hirata, H. Moshhammer, and F. Ruggiero, Particle Accelerators 40, 205 (1993).
- [5] S. Krishnagopal and R. Siemann, Phys. Rev. Lett. 67, 2461 (1991).
- [6] K. Ohmi, Phys. Rev. E 62, 7287 (2000).
- [7] Y. Cai, A. W. Chao, S. I. Tzenov, and T. Tajima, Phys. Rev. ST Accel. Beams. 4, 011001 (2001).
- [8] J. Qiang, M. Furman, and R. Ryne, Phys. Rev. ST Accel. Beams 5, 104402 (2002).
- [9] E. B. Anderson and J. T. Rogers, in Proceedings of a Workshop on beam-beam effects in circular colliders, edited by T. Sen and M. Xiao (2001), vol. FERMILABConf-01/390-T, p. 136.
- [10] Y. Zhang, K. Ohmi, and L. Chen, Phys. Rev. ST-AB 8, 074402 (2005).
- [11] X. Buffet, private communications (2015).
- [12] M. P. Zorzano and F. Zimmermann, Phys. Rev. ST-AB 3, 044401 (2000).
- [13] K. Ohmi, K. Hirata, K. Ohmi, Phys. Rev. E49, 751 (1994).
- [14] Y. Seimiya et al., Progress of Theoretical Physics 127, 1099 (2012).
- [15] D. Zhou et al., in this proceeding.
- [16] K. Takayama et al. Phys. Rev. Lett. 88, 144801 (2002).
- [17] F. Ruggiero and F. Zimmermann, Phys. Rev. ST-AB 5, 061001 (2002).
- [18] P. Raimondi, proceedings of the 2nd SuperB workshop, Frascati, March 2006.
- [19] M. Zobov et al., Phys. Rev. Lett. 104, 174801 (2010).

- [20] K. Ohmi, M. Tawada, Y. Cai, S. Kamada, K. Oide, and J. Qiang, Phys. Rev. ST-AB 7, 104401 (2004). [22] K. Ohmi and F. Zimmermann, Phys. Rev. ST-AB 18, 121003 (2015).
- [21] K. Ohmi, M. Tawada, Y. Cai, S. Kamada, K. Oide, and J. Qiang, Phys. Rev. Lett. 92, 214801 (2004).